

Location Specific Cell Transmission Model for Freeway Traffic^{*}

CHEN Xiqun (陈喜群), SHI Qixin (史其信), LI Li (李力)^{†,**}

Department of Civil Engineering, Tsinghua University, Beijing 100084, China;

[†] Department of Automation, Tsinghua University, Beijing 100084, China

Abstract: This paper describes a location specific cell transmission model of freeway traffic based on the observed variability of fundamental diagrams both along and across freeway segments. This model extends the original cell transmission model (CTM) mechanism by defining various shapes of fundamental diagrams to reproduce more complex traffic phenomena, including capacity drops, lane-by-lane variations, nonhomogeneous wave propagation velocities, and temporal lags. A field test on a Canadian freeway was used to demonstrate the validity of the location specific CTM. The simulated spatio-temporal evolutions of traffic flow show that the model can be used to describe the traffic dynamics near bottlenecks more precisely than the original model.

Key words: cell transmission model (CTM); freeway traffic; fundamental diagram

Introduction

The study of macroscopic continuum traffic flows began with the well known Lighthill-Whitham-Richards (LWR) model which was proposed independently by Lighthill and Whitham in 1955^[1] and Richards in 1956^[2]. The model assumes that the discrete flow of vehicles can be approximated by a continuous flow and then vehicle dynamics can be described by the spatial vehicle density $\rho(x, t)$ as a function of the freeway location, x , and time, t . As a result, many theoretical and numerical methods can be used to study this property based on the partial differential equation type traffic flow model.

The cell transmission model (CTM) was proposed by Daganzo^[3,4] as a direct discretization of the LWR model using the Godunov Scheme^[5], in which the flow rate is modeled as a function of density with a triangular or trapezoidal form. Different modifications of the CTM have been proposed in the last decade. For example, lags were introduced to formulate the lagged cell transmission model (LCTM) that adopts a nonconcave fundamental diagram, with consideration of the fact that the forward wave velocity is larger than the backward wave velocity^[6]. Another approach is the wave tracking resolution scheme based on the iterative construction of the exact solution of the fundamental diagram^[7]. In some recent approaches, extensions of CTM have combined various higher order traffic flow models to reproduce nonlinear spatial-temporal phenomena (e.g., shock waves, rarefaction waves, stop-and-go waves, and local cluster effects) on freeways^[8-12]. Other modifications include the switching state model (SSM)^[13], asymmetric cell transmission model (ACTM)^[14], and compositional CTM^[15].

This paper presents a modified CTM, named the location specific cell transmission model, which emphasizes the dependence of the model parameters on the

Received: 2009-04-23; revised: 2010-05-21

^{*} Supported in part by the National Key Basic Research and Development (973) Program of China (No. 2006CB705506), the National Natural Science Foundation of China (No. 50708055), the Key Technologies Research & Development Program of the Eleventh Five-Year Plan of China (No. 2007BAK35B06), and the Scientific Research Foundation for the Returned Overseas Chinese Scholars, Ministry of Education

^{**} To whom correspondence should be addressed.

E-mail: li-li@mail.tsinghua.edu.cn; Tel: 86-10-62782071

properties of the road segments. The diverse traffic characteristics are examined both lane-by-lane and site-by-site based on empirical data. The temporal lag effects of the CTM are also calculated for all the sections using different shaped fundamental diagrams along the freeways.

1 Cell Transmission Model

1.1 Basic model

Table 1 shows the parameters and variables used to formulate the model in this paper. Generally, the mass conservation in fluid dynamics can be written as

$$\rho_t(x, t) + q_x(x, t) = g(x, t) \tag{1}$$

where subscripts denote partial derivatives, $\rho(x, t)$ is the density at position, x , and time, t ; $q(x, t)$ is the flow rate; and $g(x, t)$ is the net traffic inflow.

Table 1 Model parameters and variables

Symbol	Definition	Typical value	Unit
q_m	Mainline capacity	1800-2000	veh/(h·lane)
q_{mc}	Mainline maximum congested flow	1600-1800	veh/(h·lane)
v_f	Free flow speed	100-120	km/h
w	Congestion wave speed	30-40	km/h
ρ_c	Critical density (free flow to congestion)	20-30	veh/km
ρ_{cc}	Critical density (congestion to free flow)	20-30	veh/km
ρ_{jam}	Jam density	130-160	veh/km
ρ_d	Density of queue dissipation	Variable	veh/km
ρ_q	Density of queue formation	Variable	veh/km
$f_i(t)$	Flow from section i to $i-1$ in period t	Variable	veh/(h·lane)
$R_i(t)$	On-ramp flow of section i in period t	Variable	veh/(h·lane)
$S_i(t)$	Off-ramp flow of section i in period t	Variable	veh/(h·lane)
$\rho_i(t)$	Density in section i in period t	Variable	veh/km

The LRW model assumes that the system is in equilibrium, so $q(x, t) = \rho(x, t)V_c(\rho) = Q_c(\rho)$. Equation (1) can be rewritten as

$$\rho_t(x, t) + f_\rho(\rho) \rho_x(x, t) = g(x, t) \tag{2}$$

The CTM discretizes the time and space scales in Eq. (2) to obtain a mainline flow conservation equation in

section i as

$$y_i(t+1) = y_i(t) + f_{i-1}(t) - f_i(t) + R_i(t) - S_i(t) \tag{3}$$

where $y_i(t)$ is the number of vehicles in cell, i , in period, t ; $f_i(t)$ is the number of vehicles transferring from cell, i , to $i+1$ in period, t ; and $R_i(t)$ and $S_i(t)$ are the on- and off-ramp flows.

The flow is assumed to be constant during each time step, which can easily be calculated by

$$f_i(t) = \min\{S[\rho(i, t)], R[\rho(i+1, t)]\} = \min\{Q_c[\rho(i, t)], Q_c[\rho(i+1, t)], q_m\} \tag{4}$$

where S and R are sending and receiving functions that reflect the relationship between the demand of downstream cell, i , and the supply of upstream cell, $i+1$. Different $Q_c(\rho)$ can be defined here, which lead to different CTMs. However, the fundamental diagram is correlative with the feature of flow in each segment being a function of geometric characteristics, speed limits, and ramp metering.

1.2 Location specific CTM model

The original CTM model assumes a continuous fundamental diagram. However, the phenomena of capacity drop and induced discontinuities in the density-flow relationship often appear at merging bottlenecks on freeways. Therefore, the maximum saturated flow during congestion, known as the queue discharge rate, is often smaller than the true capacity. The more accurate model uses a piecewise linear assumption for the fundamental diagram for the sake of simplicity.

For the extensive version of the CTM, the freeway is divided into N cells, some of which contain one on-ramp and/or one off-ramp as shown in Fig. 1. Freeway sections are numbered from 0 to $N-1$ starting from the most upstream cell.

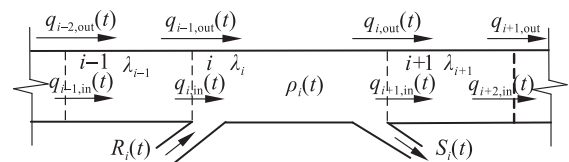


Fig. 1 Freeway with one on-ramp and/or one off-ramp

The conservation equation is directly derived from the LRW model as

$$\rho_i(t + \Delta t) = \rho_i(t) + \frac{\Delta t}{\lambda_i l_i} [q_{i-1,i}(t) - q_{i,i+1}(t)] = \rho_i(t) + \frac{\Delta t}{\lambda_i l_i} [q_{i,in}(t) - q_{i,out}(t)] \tag{5}$$

where i denotes the cell number; Δt is the time interval; l_i is the cell length, i ; λ_i is the number of lanes in cell, i ; $\rho_i(t)$ is the vehicle density in cell, i ; at time, t ; and $q_{i,in}(t)$ and $q_{i,out}(t)$ denote the traffic flows entering and leaving cell, i , at time, t .

The original LWR model is extended by dividing the traffic states into a free flow (F) and a congestion flow (C). The corresponding state transition density in the field data for the free flow is ρ_q while that for the congestion flow is ρ_d . Regressions of field data show that a critical density, ρ_c , can be defined such that the F→C phase transition occurs for $\rho(x,t) > \rho_c$ and for $q(x,t)/\rho(x,t) < v_T(x,t)$, the phase transition speed is $v_T(x,t) = [q_q(x,t) - q_d(x,t)] / [\rho_q(x,t) - \rho_d(x,t)]$. Similarly, a regressive critical density ρ_{cc} can be defined to trigger the C→F phase transition for $\rho(x,t) < \rho_{cc}$ and $q(x,t)/\rho(x,t) > v_T(x,t)$.

Thus, the piecewise linear CTM is written as:

if $\rho(x,t) \leq \rho_c(x,t)$,

$$Q_e[\rho(x,t)] = \max\{v_f(x,t)\rho(x,t), q_m\} \quad (6a)$$

if $\rho_c(x,t) < \rho(x,t) \leq \rho_{cc}(x,t)$,

$$Q_e[\rho(x,t)] = q_{mc} \quad (6b)$$

if $\rho(x,t) > \rho_{cc}(x,t)$,

$$Q_e[\rho(x,t)] = \max\{q_{mc} - w(x,t)[\rho(x,t) - \rho_{cc}(x,t)], q_m, q_{mc}\} \quad (6c)$$

As with the original CTM, the maximum sending flow of the upstream section is assumed to be at the free flow speed v_f but not more than the mainline capacity q_m , when the upstream cell density is low. The maximum receiving flow of the downstream cell is at the backward wave speed w but not more than the congested capacity q_{mc} , which ensures that the mainline flow does not exceed what can be accommodated by the downstream cell.

Thus, if no data were collected at the on-ramp i , the on-ramp flow $R_i(t)$ can be estimated as

$$R_i(t) = \gamma_i(t)q_{i,in}(t) = \gamma_i(t)[R_i(t) + q_{i-1,out}(t)] \quad (7)$$

where $\gamma_i(t)$ is the dimensionless blending ratio for the on-ramp i .

The off-ramp flow, $S_i(t)$, can be estimated by

$$S_i(t) = \beta_i(t)q_{i,out}(t) = \beta_i(t)[S_i(t) + q_{i+1,in}(t)] \quad (8)$$

where $\beta_i(t)$ is a dimensionless split ratio for off-ramp i , defined for each cell and set to 0 if the cell does not contain an off-ramp.

The time lags of the receiving function are used to

more accurately describe the transmission as^[6]

$$f_i(t) = \min\{S[\rho(i,t)], R[\rho(i+1, t-l\Delta t)]\} = \min\{Q_e[\rho(i,t)], Q_e[\rho(i+1, t-l\Delta t)], q_m\} \quad (9)$$

where l is the lag based on $l < [l_i(\Delta t | w_i |_{\max})^{-1}]$ where $|w_i |_{\max}$ is the maximum absolute backward wave speed.

The extensive transmission criteria between cell $i-1$ and i with an on-ramp is as:

Free flow-to-free flow,

$$q_{i-1,out}(t) = \min\{q_{m,i-1}, \rho_{i-1}(t)v_{f,i-1}, \rho_{i-1}(t)\lambda_i l_{i-1} / \Delta t\} \quad (10a)$$

Congestion-to-free flow,

$$q_{i-1,out}(t) = \min\{q_{mc,i-1}, \rho_{i-1}(t)\lambda_i l_{i-1} / \Delta t\} \quad (10b)$$

Free flow-to-congested flow,

$$q_{i-1,out}(t) = \max\{\min\{q_{m,i-1}, q_{mc,i} - [\rho_i(t-l\Delta t) - \rho_{cc,i}]w_i - R_i(t), \rho_{i-1}(t)\lambda_i l_{i-1} / \Delta t\}, 0\} \quad (10c)$$

Congested flow-to-congested flow,

$$q_{i-1,out}(t) = \max\{\min\{q_{mc,i-1}, q_{mc,i} - [\rho_i(t-l\Delta t) - \rho_{cc,i}]w_i - R_i(t), \rho_{i-1}(t)\lambda_i l_{i-1} / \Delta t\}, 0\} \quad (10d)$$

The transmission rules for the off-ramp cells are similar. For the conservation of flow at the boundary between two cells,

$$q_{i,in}(t) = q_{i-1,out}(t) + R_i(t) \quad (11a)$$

$$q_{i+1,in}(t) = q_{i,out}(t) - S_i(t) \quad (11b)$$

2 Dependence of Model Parameters on Sensor Location

The section uses the loop data collected from the I5 freeway in California to show the dependence of model parameters on the sensor location. The data was collected by the loop-detector with an aggregation time window length of 5 min from Nov. 1 to Nov. 30, 2008^[16].

2.1 Lane-by-lane variability of density-flow relationship

Figure 2 shows the significant traffic flow differences for five lanes at the same location on the I5 freeway. Lanes 1 and 2 exhibit the reverse- λ shape fundamental diagrams with obvious capacity drop. Lanes 3 and 4 have triangle density-flow relationships with two distinct regimes of free flow and homogeneous congestion flow. Lane 5 is a trapeziform fundamental diagram. All lanes have chaotic transitions between the free

flow state and the congested flow state. Lane changing maneuvers will easily cause the traffic in the right lane (i.e. Lane 5) to become congested. This clearly reflects the lane-by-lane variability of the density-flow relationship.

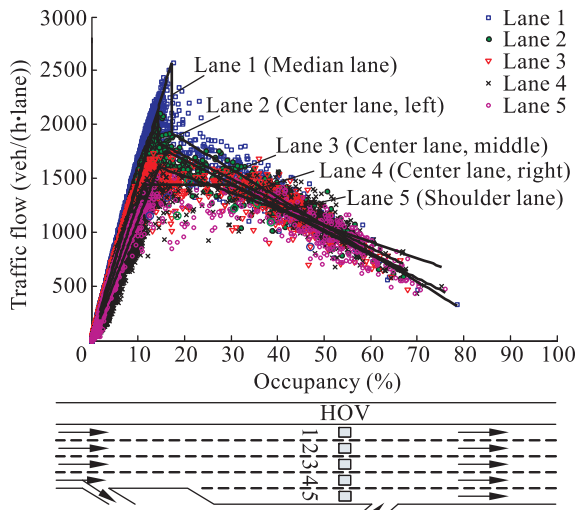


Fig. 2 Fundamental diagram for all lanes at station 1108507, 15 Freeway, California, Nov. 1-30, 2008

2.2 Site-by-site wave speed variability

Regressions for the four different segments of the 15 freeway also show that the estimated free flow speeds are almost the same at different locations, which shows that free traffic flow spreads downstream without location-based variations.

However, the data shows that congestion flows propagate upstream with different wave speeds, varying from 12 km/h to 18 km/h. These variations are related to the various shapes of the fundamental diagrams. Therefore, the wave speed, w , in the CTM receiving function should not be taken as constant along a homogenous freeway with ramps, but different model parameters should be used for different sections to improve the estimates.

3 Model Evaluation

This section shows how the modified CTM can reproduce the dynamic behaviors of real traffic flows. The testing segment along a 10-km stretch of the Queen Elizabeth Way^[17] shown in Fig. 3 had 15 loop detector stations, with the last 7 stations used to validate the model. The test stretch was subdivided into 8 cells, each with an approximate length of 650 m, with

simulation update times of $\Delta t = 20$ s. The traffic flow, occupancy, and average vehicle speed were collected every 20 s for 4 h from 6:00 am to 10:00 am. The ramp flows $R(t)$ and $S(t)$ were manually counted. The study was restricted to those days which had sufficient levels of congestion (observations in the congested regime) so that the density-flow parameters can be reliably estimated.

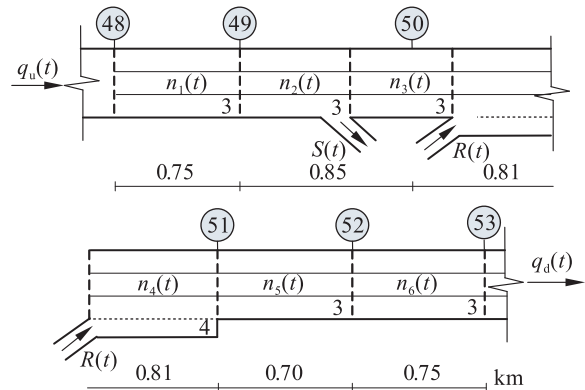


Fig. 3 Field test on Queen Elizabeth Way, Ontario, Canada

The simulated cell partition size was set to about 125 m with a simulation update time $\Delta t = 4$ s to analyze the spatio-temporal evolution of the traffic jams in detail. The analysis assumed a uniform traffic flow distribution in 20 s, and the traffic flows at stations 49-52 were unknown with the fundamental diagram parameters for these sections estimated from the data in Table 2.

Table 2 Model parameters estimated from traffic data for Queen Elizabeth Way from 6:00 am to 10:00 am, Dec. 15, 1998

Station No.	k_c %	k_{cc} %	v_f h ⁻¹	w h ⁻¹	q_m veh/(h·lane)	q_{mc} veh/(h·lane)
41	12.4	12.4	161.7	11.9	2000	1508.2
42	12.9	12.9	149.9	28.1	1940	1936.3
43	14.1	14.1	147.5	25.9	2080	1907.2
44	11.7	16.0	188.7	34.4	2200	2200.0
45	15.0	15.0	153.0	37.7	2290	2206.4
46	15.4	15.4	149.6	25.7	2310	2099.5
47	14.7	14.7	149.3	33.3	2190	2063.4
48	13.5	13.5	176.4	34.9	2390	2288.3
49	12.6	12.6	188.9	32.2	2380	2164.9
50	13.6	13.6	158.4	21.0	2160	1994.6
51	18.3	18.3	133.2	13.8	2440	2252.7
52	16.8	16.8	139.1	25.8	2330	1952.0
53	18.4	18.4	129.4	21.0	2380	2285.7

The models were evaluated by reconstructing the flows at stations 48-52 using the CTM data upstream station 48 and downstream station 53. The measured

and simulated time occupancies are compared in Fig. 4.

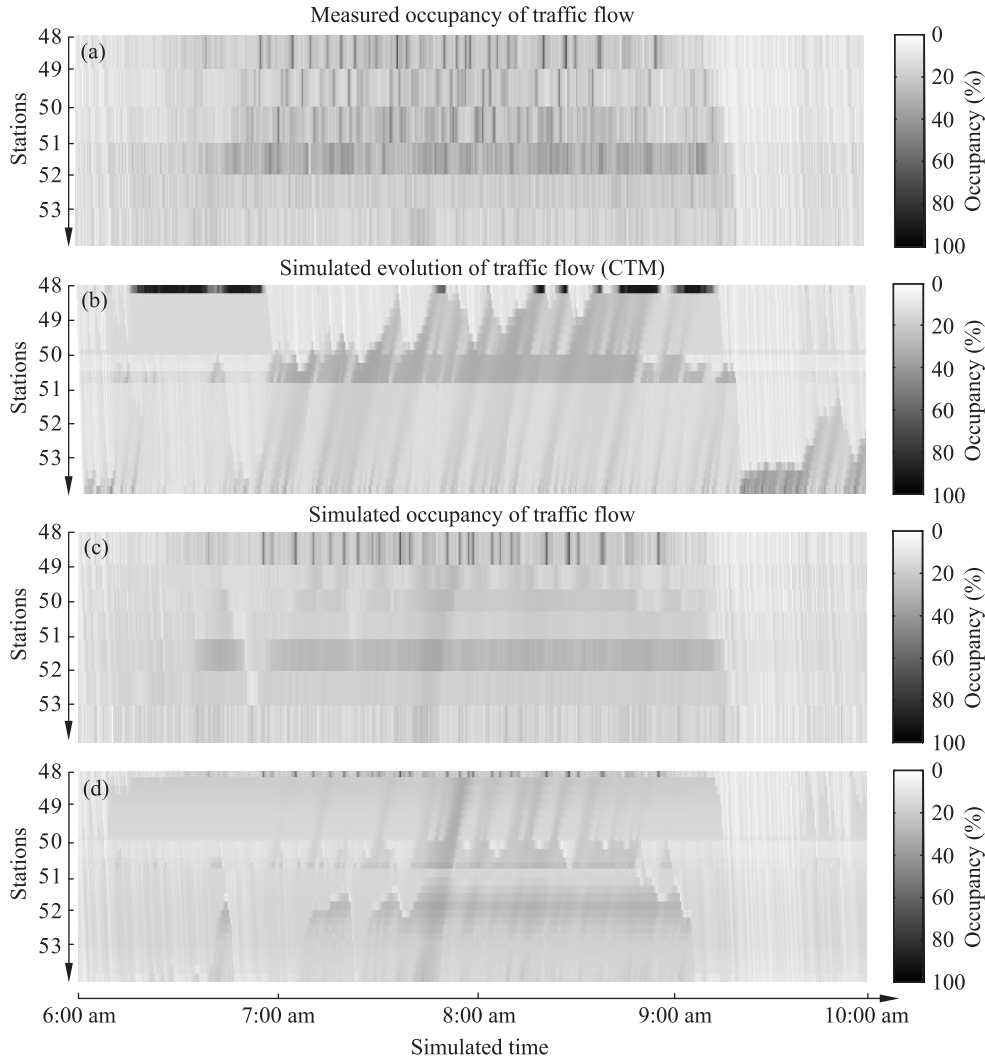


Fig. 4 Measured and predicted spatio-temporal occupancy evolution for 6:00 am to 10:00 am where Station 53 is at the bottom of each figure and Station 48 is at the top. (a) Field data, (b) CTM with $\Delta t = 4$ s; (c) LS-CTM with $\Delta t = 20$ s; (d) LS-CTM with $\Delta t = 4$ s.

Figure 4a shows the measured traffic flow evolution. Figure 4b shows the simulation results of the original CTM that assumes a uniform parameter set for the fundamental diagram of $q_m = 2390$, $q_{mc} = 2130$, $k_c = 13.1\%$, $k_{cc} = 13.1\%$, $v_f = 182.8$, and $w = 24.5$. The congestion wave propagates upstream with the proper velocity with the bottleneck exaggerated identified near the on/off ramps. Figures 4c and 4d show that the backward-traveling shock wave emanating from the bottleneck near Station 51 after about 6:40 am travels faster than the forward-traveling shock

(dissipation wave). A wide moving jam is triggered to propagate backward from Station 53 at about 7:40 am. These features observed on the freeway are correctly reproduced by the model but not by the original CTM. Thus the location specific CTM accurately reproduces the observed bottlenecks and the approximate duration and spatial extent of the congestion upstream of each bottleneck. The accuracy of the estimated spatio-temporal dynamics illustrates the effectiveness of this method, even with noise and fluctuations.

4 Conclusions

Field data were used to calculate both lane-by-lane and site-by-site variations of the traffic flow parameters for a fundamental diagram model of freeway traffic flows. A modified CTM model was then used to take into account the model variability influenced by sensor locations, geometry features, and many other factors. The lane-by-lane fundamental diagrams show obvious variations, where the free flow speed decreases from the median lane (high occupancy vehicle lane) to the shoulder lane and the capacity drop only exists on the median two lanes from the experimental segment on the I5 Freeway, California. Field tests demonstrate that the predictions by the modified CTM better fit the field data. The model can be further applied to on-line incident detection, routing, and ramp metering control due to its piecewise linear transmission structures.

References

- [1] Lighthill M J, Whitham G B. On kinematic waves: II. A theory of traffic flow on long crowded roads. *Proceedings of the Royal Society of London, Series A*, 1955, **229**(1178): 317-345.
- [2] Richards P I. Shockwaves on the highway. *Operations Research*, 1956, **4**(1): 42-51.
- [3] Daganzo C F. The cell transmission model: A dynamic representation of highway traffic consistent with the hydrodynamic theory. *Transportation Research, Part B, Methodology*, 1994, **28**(4): 269-287.
- [4] Daganzo C F. The cell transmission model—Part II: Network traffic. *Transportation Research, Part B, Methodology*, 1995, **29**(2): 79-93.
- [5] Lebacque J P. The Godunov scheme and what it means for first order traffic flow models. In: *Transportation and Traffic Theory*. New York: Pergamon-Elsevier, 1996: 647-677.
- [6] Daganzo C F. The lagged cell transmission model. In: *The 14th International Symposium on Transportation and Traffic Theory*. Jerusalem, Israel, 1999: 147-171.
- [7] Henn V. A wave-based resolution scheme for the hydrodynamic LWR traffic flow model. In: *Traffic and Granular Flow'03*. Berlin Heidelberg: Springer-Verlag, 2005: 105-124.
- [8] Gomes G, Horowitz R, Kurzhanskiy A A, et al. Behavior of the cell transmission model and effectiveness of ramp metering. *Transportation Research, Part C, Emerging Technologies*, 2008, **16**(4): 485-513.
- [9] Payne H J. Models of freeway traffic and control. In: Bekey G A, ed. *Mathematical Models of Public Systems*, 1971: 51-61.
- [10] Papageorgiou M, Blosseville J M, Haj-Salem H. Modelling and real-time control of traffic flow on the southern part of Boulevard Périphérique in Paris — Part I: Modelling. *Transportation Research, Part A, Policy*, 1990, **24**: 345-359.
- [11] Jiang R, Wu Q S, Zhu Z J. A new continuum model for traffic flow and numerical tests. *Transportation Research, Part B, Methodology*, 2002, **36**: 405-419.
- [12] Wang Y B, Papageorgiou M, Messmer A. Real-time freeway traffic state estimation based on extended Kalman filter: Adaptive capabilities and real data testing. *Transportation Research, Part A, Policy*, 2008, **42**(6): 1340-1358.
- [13] Muñoz L, Sun X, Sun D, et al. Methodological calibration of the cell transmission model. In: *Proceedings of American Control Conference*. Boston, MA, 2004: 798-803.
- [14] Gomes G, Horowitz R. Optimal freeway ramp metering using the asymmetric cell transmission model. *Transportation Research, Part C: Emerging Technologies*, 2006, **14**(4): 244-262.
- [15] Boel R, Mihaylova L. A compositional stochastic model for real time freeway traffic simulation. *Transportation Research, Part B, Methodology*, 2006, **40**(4): 319-334.
- [16] PeMS. [Http://pems.eecs.berkeley.edu/](http://pems.eecs.berkeley.edu/), 2009.
- [17] Mauch M, Cassidy M J. Freeway traffic oscillations: Observations and predictions. In: *The 15th International Symposium on Transportation and Traffic Theory*. Oxford, UK, 2002: 653-674.